DE GRUYTER

J. Appl. Geodesy 2017; 11(2): 107–114

Luis García-Asenjo*, Sergio Baselga, Pascual Garrigues

# Deformation Monitoring of the Submillimetric UPV Calibration Baseline

**Abstract:** A 330 m calibration baseline was established at the *Universitat Politècnica de València* (UPV) in 2007. Absolute scale was subsequently transferred in 2012 from the Nummela Standard Baseline in Finland and distances between pillars were determined with uncertainties ranging from 0.1 mm to 0.3 mm. In order to assess the long-term stability of the baseline three field campaigns were carried out from 2013 to 2015 in a co-operative effort with the *Universidad Complutense de Madrid* (UCM), which provided the only Mekometer ME5000 distance meter available in Spain. Since the application of the ISO17123-4 full procedure did not suffice to come to a definite conclusion about possible displacements of the pillars, we opted for the traditional geodetic network approach. This approach had to be adapted to the case at hand in order to deal with problems such as the geometric weakness inherent to calibration baselines and scale uncertainty derived from both the use of different instruments and the high correlation between the meteorological correction and scale determination. Additionally, the so-called the maximum number of stable points method was also tested. In this contribution it is described the process followed to assess the stability of the UPV submillimetric calibration baseline during the period of time from 2012 to 2015.

**Keywords:** Deformation Monitoring, Calibration Baseline, Distancemeter (EDM), Mekometer ME5000

---

**\*Corresponding author: Luis García-Asenjo,** Department of Cartographic Engineering, Geodesy and Photogrammetry, Universitat Politècnica de València, Camino de Vera s/n, 46022 Valencia, Spain, e-mail: lugarcia@upv.es, http://orcid.org/0000-0001-6535-2216
**Sergio Baselga,** Department of Cartographic Engineering, Geodesy and Photogrammetry, Universitat Politècnica de València, Camino de Vera s/n, 46022 Valencia, Spain, e-mail: serbamo@cgf.upv.es, http://orcid.org/0000-0002-0492-4003
**Pascual Garrigues,** Department of Cartographic Engineering, Geodesy and Photogrammetry, Universitat Politècnica de València, Camino de Vera s/n, 46022 Valencia, Spain, e-mail: pasgarta@cgf.upv.es

## 1 Introduction

GNSS techniques have shown a promising potential for determining distances in the order of hundreds of meters with uncertainties below one millimeter [1, 15]. Research in the field of submillimetric GNSS length determination requires the use of outdoor metrological infrastructures traceable to the SI-meter with an accuracy of some tenths of a millimeter [9, 10, 14, 17, 19].

Those metrological infrastructures, also called calibration baselines, consist traditionally of a number of alligned pillars which relative distances are known. Those pillars are then used as reference marks for subsequent distance comparisons according to ISO 17123-4 [11]. In our case, the UPV calibration baseline is used to compare GNSS-based distances with distances measured using electronic distance meters (EDM) such as the submillimetric Mekometer ME5000 [4].

In 2012, the inter-pillar distances of the UPV calibration baseline were traced to SI-metre using a Mekometer ME5000 calibrated at the Nummela Standard Baseline [12, 13, 16]. This scale transfer, performed by the Finnish Geospatial Research Institute (FGI), produced a set of FGI-certified distances with uncertainties ranging from 0.1 mm to 0.3 mm.

However, for subsequent comparisons between both GNSS-based and FGI-certified distances, possible pillar displacements must be taken into account. Besides, deformation monitoring also allows us to know which are the most stable pillars so that optimal selection can be planned in advance to conduct the GNSS absolute length research at the UPV baseline [3].

Consequently, three field campaigns were carried out respectively in 2013, 2014 and 2015 using similar type of equipment and observational scheme as the original campaign in 2012, though different instruments. In addition, horizontal deformation monitoring could be attempted using the traditional geodetic network approach [6, 18] since the UPV baseline has one not-aligned seventh pillar.

Nonetheless, there are some drawbacks in this deformation monitoring process: firstly, the suspected movements between epochs tend to be rather small if compared

to the uncertainty of the measurements (0.5 mm vs. 0.2–0.3 mm); secondly, the geometry of calibration baselines as geodetic networks is intrinsically weak; thirdly, a proper set of calibration parametres i. e. additive constant **a** and scale correction **b**, has to be determined for each campaign in order to realize the SI-metre distances traced in 2012; finally, displacement of pillars, refraction errors and calibration parameters are highly correlated.

In the following, the effort to overcome the above mentioned drawbacks in order to obtain a reliable assessment of possible displacement of the UPV baseline pillars is summarized. First, the UPV calibration baseline and the technical details of the four measurement campaigns are described respectively in section 2 and section 3. In the following sections, the process for obtaining the calibration parameters for each campaign (section 4), the deformation monitoring using both the classical geodetic network approach (section 5) and maximum number of stable points method (section 6) are discussed. Finally, some conclusions are given.

## 2 The UPV Calibration Baseline

The UPV calibration baseline was set up by the Department of Cartographic Engineering, Geodesy and Photogrammetry (DICGF) in November 2007 as a part of a triangle-shaped test field (see Figure 1) initially planned to evaluate the uncertainty of geodetic instruments and their ancillary equipment according to ISO 17123 series [5].

The calibration baseline consists of six observation pillars (No. 1 to No. 6) approximately in line at 0, 28, 94, 198, 282 and 330 m, following the Heerbrugg-type design [20]. All pillars have a diameter of 22 cm and heighten 1.20 m above ground level. They consist of two insulated steel pipes, the inner one covering a concrete structure
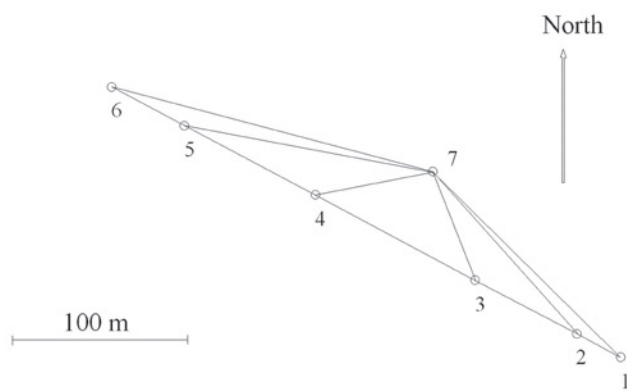


**Figure 2:** Pillar perspective.

with one square metre foundation that extends to a depth of 60 cm. The outer steel pipe prevents the inner pillar from differential dilations due to meteorological effects. They have a double forced-centering mount system to install measuring instruments on the top: the standard 5/8" fixing screw and the Kern-type trivet system (Figure 2).

The terrain in which the test field was built has a uniform geological profile with the layers reaching the following depths: thin topsoil over sandy gravels to 1.2 m; inorganic sandy muds of low plasticity to 2.1 m; brown silty-sandy clay, medium and low plasticity to 3.8 m; water table at 3.8 m; organic grey silty clay, medium and low plasticity to 5.5 m; sandy graves to 13.6 m.

According to the geological profile the pillars were expected to be stable after a settling time. Three measurement campaigns were carried out from December 2007 to February 2008 using the following total stations: Topcon GTS605, Leica TPS 1200+ and Leica TDA5005. All of them proved to be compatible within a combined least squares adjustment and the coordinates given in Table 1 were adopted as first set of approximate local coordinates.

**Table 1:** Set of approximate 3D local coordinates (2008) and their corresponding standard deviations given in the local geodetic system of pilar 1. The third coordinate z refers to the top of the pillar.

| Pillar | x(m) | $\sigma_x$(mm) | y(m) | $\sigma_y$(mm) | z(m) | $\sigma_z$(mm) |
|---|---|---|---|---|---|---|
| 1 | 0.000 | 0.0 | 0.000 | 0.0 | 0.000 | 0.0 |
| 2 | 28.379 | 0.4 | −0.162 | 2.7 | 0.019 | 0.3 |
| 3 | 94.396 | 0.4 | 0.112 | 1.9 | 0.201 | 0.3 |
| 4 | 198.003 | 0.4 | −0.132 | 2.1 | 0.206 | 0.4 |
| 5 | 282.786 | 0.4 | 0.069 | 3.2 | 0.449 | 0.4 |
| 6 | 330.004 | 0.4 | 0.000 | 0.0 | 0.313 | 0.4 |
| 7 | 144.812 | 0.5 | −43.405 | 1.8 | 0.042 | 0.3 |



**Figure 1:** Triangle-shaped test field and the UPV calibration baseline (pillars No. 1 to No. 6).

Unfortunatelly, two facilities installed in 2010 obstructed the visibility for lines 2–7 and 5–7, and as a result the pillar No. 7 could only be linked to the calibration baseline through lines 1–7, 3–7, 4–7 and 6–7, thus weakening even more the network.

In order to detect possible vertical displacements of pillars, a field campaign was carried out in 2013 using both geometric and trigonometric high precision levelling methods. Since no significant vertical displacement was detected, the original vertical coordinates obtained in 2008 were safely regarded for subsequent computations.

# 3 Description of the EDM Field Campaigns

Although the first campaign aimed primarily the determination of the traced to SI-metre inter-pillar distances of the UPV calibration baseline, it was also used as starting campaign for deformation monitoring purposes.

The three subsequent campaigns, carried out respectively in 2013, 2014 and 2015, followed the same operational scheme with similar type of EDM, *i. e.* Mekometer ME5000, though different instruments.

The operational scheme consisted in four sets of 'double-in-all-combinations' distances. Except line 1–7, which only could be measured 8 times forwards, every distance was measured 16 times which gave rise to 296 measured distances for each campaign. The EDM and the reflector were installed in the 5/8" fixing screws of the pillars using two Leica GDF321 tribrachs.

Regarding meteorological instruments, dry and wet temperatures were measured using calibrated Thies Clima Assmann-Type psycrhometers with an estimated ±0.3 °C uncertainty. Air pressure was measured using two calibrated Thommen 3B4.01.1 aneroid barometers with an estimated ±0.3 hPa uncertainty. Two parasoles were always used to shade all the measurement equipment in both ends of the beam path.

The main facts of each campaign are summarized as follows.

The first field campaign was carried out in 2012, from May 28 to June 1, including specialists from both FGI and UPV. The measurements were done using the Mekometer ME5000 of the Aalto University (No. 357094) along with the reflector (No. 374414). Weather during the measurements was mostly sunny, temperatures ranged from +21.0 °C to +27.0 °C, air pressures from 1012.8 hPa to 1019.8 hPa and relative humidities from 42 % to 77 %.

All the subsequent campaigns were measured in agreement with the UCM which also supplied their Mekometer ME5000 (No. 357094) and similar meteorological instruments as those used in the first campaign by the FGI.

The second field campaign was carried out in 2013 from June 25 to June 28 using the reflector No. 374448. Weather during the measurements was not so stable as it was in the first campaign. Although it was mostly sunny, some series were measured under cloudy and windy conditions. Temperatures ranged from +19.8 °C to +25.2 °C, air pressures from 1021.2 hPa to 1023.4 hPa and relative humidities from 51 % to 80 %.

The third campaign was carried out in 2014 from June 25 to June 28. The measurements were done using the reflector No. 374447. Weather during the measurements was fairly stable. Temperatures ranged from +21.9 °C to +28.1 °C, air pressures from 1011.4 hPa to 1017.1 hPa and relative humidities from 44.8 % to 82.2 %.

The fourth campaign was carried out in 2014 from July 21 to July 24. The measurements were done using the same reflector (No. 374447) that was used in 2014. Weather during the measurements was fairly stable. Temperatures ranged from +24.4 °C to +31.2 °C, air pressures from 1008.1 hPa to 1015.8 hPa and relative humidities from 53.8 % to 86.1 %.

# 4 Determination of the Calibration Parametres for Each Campaing

A set of calibration parametres, *i. e.* additive constant **a** and scale correction **b**, had to be determined for each campaign in order to realize the FGI-certified distances, which in turn were traced to SI-metre through the Nummela Standard Baseline in 2012.

The additive constant for each campaign was computed following the full procedure described in the ISO-17123(4) (see Table 2).

**Table 2:** Additive constant **a** obtained using the full procedure of ISO-17123(4) and scale correction **b** using the 2D geodetic network approach with the inclusion of a scale parameter.

| Year | EDM | RFL | a (mm) | b (ppm) |
|------|-----|-----|--------|---------|
| 2012 | FGI | 374414 | 0.008 ± 0.016 | 0.004 ± 1.374 |
| 2013 | UCM | 374448 | 0.121 ± 0.017 | 2.388 ± 1.459 |
| 2014 | UCM | 374447 | 0.078 ± 0.015 | 1.717 ± 1.400 |
| 2015 | UCM | 374447 | 0.056 ± 0.018 | 2.185 ± 1.766 |

The value obtained for year 2012 totally agreed with the value provided by the FGI following an independent computation process. Those obtained for the reflector No. 374447, which was used in years 2014 and 2015, can be considered statistically the same, and they differ clearly from the additive constant obtained for the reflector No. 374448, which was used in 2013. Moreover, the standard deviation of the four obtained additive constants are similar, thus reflecting that distances were measured with the same precision every year.

In addition to the additive constant, the ISO-17123(4) also yields a set of adjusted inter-pillar distances for each campaign. By inspecting the differences between the adjusted distances and their corresponding FGI-certified (see Table 3), it is apparent that some displacement have happened between campaigns. For instance, pillars No. 2 and No. 3 seem to have been displaced progressively over one millimeter from 2012 to 2015. Unfortunately, no definite conclusion about which specific pillars may have been displaced can be drawn because a number of possible individual pillar displacement may give rise to similar differences.

Since no information about scale can be obtained from the ISO-17123(4) full procedure, other methods have to be used to obtain the scale correction parameter **b.** This parameter **b** should not be considered a scale correction in a metrological sense but only a reasonable strategy to avoid the scale influence on the determined displacements.

Two different approaches were intended to obtain the scale correction parameter for each campaign. Both approaches are based on a 2D network adjustment of the measured distances assuming the additive constant **a** to be known. In the first approach **b** is included as an unknown in the network solution, whilst in the second approach **b** is obtained by means of a 2D Helmert transformation.

Although both approaches gave similar results, we retained those corresponding to the first approach (see Table 2) for subsequent computations since their standard deviation was slightly small. Even so, they are necessarily high because uncertainties of 0.2–0.3 mm in the measured distances can easily have an impact of 1–2 ppm, for the longest inter-pillar distance is only 330 m.

Additionally, the second approach revealed two interesting facts: first, 2D network solutions for years 2013, 2014 and 2015 could be transformed into the solution for year 2012 by similarity transformations whose parameters, excluding scale, were no significant even though the 2D networks solutions were obtained after 2 or more iterations; second, the experimental standard deviation of the average coordinates of the four 2D network solutions after their transformation into the 2012 frame were over 0.5 mm on average. As a consequence, the mean coordinates of the four 2D network solutions were retained as initial coordinates for subsequent computations for deformation monitoring.

# 5 Deformation Monitoring by Using the Classical Geodetic Network Approach

Taking advantage of the existence of a not-aligned seventh pillar, possible displacement of the UPV baseline pillars can be analysed using the classical geodetic network approach.

**Table 4:** Coordinate displacements obtained using the traditional geodetic approach (mm).

| Coordinate | 12–13 | 13–14 | 14–15 | 12–14 | 13–15 | 12–15 |
|---|---|---|---|---|---|---|
| X1 | −0.39 | 0.47 | −0.16 | 0.08 | 0.32 | −0.08 |
| Y1 | −0.70 | 0.54 | 0.19 | −0.16 | 0.74 | 0.03 |
| X2 | 0.71 | −0.04 | 0.36 | 0.67 | 0.32 | 1.03 |
| Y2 | −0.06 | 0.00 | −0.05 | −0.05 | 0.01 | −0.05 |
| X3 | 0.08 | −0.48 | 0.36 | −0.40 | −0.12 | −0.04 |
| Y3 | 0.49 | −0.23 | 0.18 | 0.27 | −0.05 | 0.44 |
| X4 | 0.47 | 0.08 | −0.19 | 0.55 | −0.11 | 0.36 |
| Y4 | −0.12 | −0.34 | 0.48 | −0.46 | 0.14 | 0.02 |
| X5 | 0.07 | −0.77 | 0.09 | −0.71 | −0.68 | −0.61 |
| Y5 | 0.02 | 0.01 | −0.03 | 0.03 | −0.03 | −0.01 |
| X6 | 0.10 | 0.67 | −0.04 | 0.77 | 0.63 | 0.73 |
| Y6 | −0.19 | 0.44 | 0.19 | 0.25 | 0.63 | 0.44 |
| X7 | −1.03 | 0.07 | −0.42 | −0.96 | −0.35 | −1.38 |
| Y7 | 0.56 | −0.43 | −1.00 | 0.13 | −1.43 | −0.88 |

**Table 3:** Independent inter-pillar distances obtained using the full procedure of ISO-17123(4) minus FGI-certified distances (mm). All the computed standard uncertainties (k=1) ranged from 0.189 to 0.205. Please note that distances for year 2012 totally agree with the FGI-certified ones despite having followed an independent computing process.

| Line | 2012 | 2013 | 2014 | 2015 |
|---|---|---|---|---|
| 1–2 | −0.00 | 1.04 | 0.54 | 1.05 |
| 2–3 | −0.01 | −0.78 | −1.18 | −1.22 |
| 3–4 | −0.01 | 0.13 | 0.77 | 0.17 |
| 4–5 | −0.01 | −0.61 | −1.40 | −1.16 |
| 5–6 | 0.01 | −0.07 | 1.40 | 1.25 |

Although detection of small movements by means of rigorous mathematical procedure is a well documented problem in geodesy [6, 8, 18], the case at hand has to cope, among other problems mentioned in the first section, with the inherent weak geometry of calibration baselines due to the alignment of pillars.

Even with the inclusion of the existing not-aligned seventh pillar, the standard deviation of the y-coordinates obtained in the free-network solutions ranges from 1.6 mm to 7.7 mm, thus impeding the detection of movements which are expected to be near 0.5 mm. As a consequence, the ill-conditioned system of equations was regularized under the hypothesis of possible displacements of 0.5 mm from the initial average coordinates obtained as described in section 4. Aside from testing the global matematical model, all residuals, including those concerning regularization, were individually tested using both Baarda and Pope's tests.

Since average distances for each line were used as observables and only 14 coordinate parameters had to be solved, all network solutions had 19 degrees of freedom. All distances were weighted using their corresponding experimental standard deviations expanded to take into account the influence of the applied calibration parameters, *i. e.* additive constant **a** and scale correction **b,** given in Table 2. Then, the system of linear equations

$$\mathbf{Ax} = \mathbf{l} + \mathbf{r} \tag{1}$$

with **A** the coefficient matrix, **x** the vector of coordinate parameters, **l** the difference between both horizontally reduced observed and computed distances, is solved as usual to obtain the network solution for epoch *i* using

$$\mathbf{x}_i = (\mathbf{A}^T\mathbf{P}_i\mathbf{A})^+ \mathbf{A}^T\mathbf{P}_i\mathbf{l}_i \tag{2}$$

with $\mathbf{P}_i$ the weight matrix. The unit weight variance $\hat{\sigma}_0^2$ is computed and the global model tested with a level of significance α = 0.01. Subsequently, the vector of residuals is checking for outlier detection.

Once the network solution for each campaign has been obtained and statistically tested, the deformation vector for each pair of solutions *i* and j is obtained using

$$\mathbf{d}_{ij} = \mathbf{x}_j - \mathbf{x}_i \tag{3}$$

with an estimated precision

$$\Sigma_{\mathbf{d}_{ij}\mathbf{d}_{ij}} = \Sigma_{\mathbf{x}_i\mathbf{x}_i} + \Sigma_{\mathbf{x}_j\mathbf{x}_j} \tag{4}$$

where **Σ** represents the corresponding covariance matrix. The coordinate displacements obtained for the different

campaign pairs using this classical geodetic approach are shown in Table 4. The corresponding standard deviations are respectively 0.25 mm ≤ σ_x ≤ 0.37 mm and 0.30 mm ≤ σ_y ≤ 0.91 mm.

Finally, once the deformation **d**-vectors were obtained, the so-called Global Congruency Test (GCT) was applied to evaluate the hypothesis of zero overall displacement using the W statistic [7, 18]

$$W = \frac{\mathbf{d}^T\mathbf{Q}_{dd}^+\mathbf{d}}{rank(\mathbf{Q}_{dd}^+)\hat{\sigma}_0^2} \tag{5}$$

with $\mathbf{Q}_{dd}^+$ the displacement cofactor matrix and $\hat{\sigma}_0^2$ the overall unit weight variance. Since W follows a Fisher distribution, the null hypothesis $H_0$: d=0 is accepted with a level of significance of α = 0.001 if $W \le F_{(14,38,0.999)} = 3.820$. Otherwise, the alternative hypothesis $H_1$: d≠0 is considered, that is to say that an overall deformation exists.

Further investigation on each single point of the network can be conducted using the same test, though only the corresponding 2D components of interest of both the **d**-vector and minor of the matrix $\mathbf{Q}_{dd}^+$ in (5) are considered. A single horizontal displacement is accepted when $W \le F_{(2,38,0.950)} = 4.071$. For the sake of conciseness, only the results of the single point displacement test for pairs 2012–2013, 2012–2014, 2012–2015, and 2014–2015 are given (see Tables 6, 7, 8 and 9).

**Table 5:** Results of the overall horizontal displacement test using the GCT for all the possible pairs.

| Years | W | $F_{(14,19,0.999)}$ | Conclusion |
|---|---|---|---|
| 2012–2013 | 3.596 | < 3.820 | No deformation |
| 2012–2014 | 18.891 | > 3.820 | DEFORMATION |
| 2012–2015 | 17.145 | > 3.820 | DEFORMATION |
| 2013–2014 | 6.868 | > 3.820 | DEFORMATION |
| 2013–2015 | 5.023 | > 3.820 | DEFORMATION |
| 2014–2015 | 4.589 | > 3.820 | DEFORMATION |

**Table 6:** Results of the single point horizontal displacement tests from 2012 to 2013.

| Pillar | δ (mm) | $\sigma_\delta$ (mm) | W | Conclusion |
|---|---|---|---|---|
| 1 | 0.80 | 0.79 | 1.0755 | No deformation |
| 2 | 0.71 | 0.97 | 2.0905 | No deformation |
| 3 | 0.50 | 0.59 | 0.5656 | No deformation |
| 4 | 0.48 | 0.57 | 0.9445 | No deformation |
| 5 | 0.07 | 0.97 | 0.0191 | No deformation |
| 6 | 0.21 | 0.85 | 0.0673 | No deformation |
| 7 | 1.17 | 0.56 | 4.6626 | DEFORMATION |

**Table 7:** Results of the single point horizontal displacement tests from 2012 to 2014.

| Pillar | δ (mm) | $\sigma_\delta$ (mm) | W | Conclusion |
|---|---|---|---|---|
| 1 | 0.18 | 0.58 | 0.1021 | No deformation |
| 2 | 0.67 | 0.72 | 3.3765 | No deformation |
| 3 | 0.48 | 0.43 | 1.5520 | No deformation |
| 4 | 0.72 | 0.42 | 3.1379 | No deformation |
| 5 | 0.71 | 0.72 | 3.7730 | No deformation |
| 6 | 0.81 | 0.63 | 4.6856 | DEFORMATION |
| 7 | 0.97 | 0.41 | 6.0940 | DEFORMATION |

**Table 8:** Results of the single point horizontal displacement tests from 2012 to 2015.

| Pillar | δ (mm) | $\sigma_\delta$ (mm) | W | Conclusion |
|---|---|---|---|---|
| 1 | 0.08 | 0.60 | 0.0438 | No deformation |
| 2 | 1.03 | 0.74 | 7.6810 | DEFORMATION |
| 3 | 0.45 | 0.45 | 0.7819 | No deformation |
| 4 | 0.36 | 0.44 | 0.9171 | No deformation |
| 5 | 0.61 | 0.74 | 2.7113 | No deformation |
| 6 | 0.85 | 0.64 | 4.2233 | DEFORMATION |
| 7 | 1.64 | 0.42 | 16.1241 | DEFORMATION |

**Table 9:** Results of the single point horizontal displacement tests from 2014 to 2015.

| Pillar | δ (mm) | $\sigma_\delta$ (mm) | W | Conclusion |
|---|---|---|---|---|
| 1 | 0.25 | 0.57 | 0.2806 | No deformation |
| 2 | 0.36 | 0.70 | 1.0586 | No deformation |
| 3 | 0.40 | 0.42 | 1.1402 | No deformation |
| 4 | 0.52 | 0.41 | 1.3462 | No deformation |
| 5 | 0.10 | 0.71 | 0.0696 | No deformation |
| 6 | 0.19 | 0.61 | 0.0677 | No deformation |
| 7 | 1.09 | 0.40 | 7.0060 | DEFORMATION |

# 6 Deformation Monitoring Under the Maximum Number of Stable Points Hypothesis

Now we want to analyze the deformation monitoring in a different light. The question of determining relative displacements in a network is an ill-posed problem with no unique solution. Infinitely many solutions in terms of possible point displacements compatible with the observed values exist. In order to obtain a solution for the corresponding rank deficient system of equations the classical geodetic procedure for relative deformation determination opts for the use of the pseudoinverse matrix. As it was previously demonstrated [2], this involves the underlying assumption that displacements, provided they occur, are expected to be small shifts (the least possible) affecting all points. This may sound as a very sensible working assumption. There are occasions, however, where displacements would rather be attributed to a single or a few number of vertices. This may be especially the case of quite unexpected, considerably large displacements where the suspicion leads to a possible movement of a single or few pillars due to unfortunate circumstances. A method to obtain the solution most compatible with the hypothesis of stability of the majority of pillars and possible large displacements in the least number of them was presented in Baselga et al. [2] and named the maximum number of stable points method.

In a nutshell, for a pair of campaigns the method solves the over-determined rank-deficient system of observation difference equations

$$\mathbf{Ad} = \mathbf{l} + \mathbf{r} \tag{6}$$

with $\mathbf{A}$ the coefficient matrix, $\mathbf{d}$ the vector of coordinate differences, $\mathbf{l}$ the difference between observations in the two campaigns and $\mathbf{r}$ the residual vector as

$$\mathbf{d} = (\mathbf{A}^\mathrm{T}\mathbf{PA})^+ \mathbf{A}^\mathrm{T}\mathbf{Pl} + (\mathbf{I} - (\mathbf{A}^\mathrm{T}\mathbf{PA})^+ (\mathbf{A}^\mathrm{T}\mathbf{PA}))\mathbf{y} \tag{7}$$

where $(\ )^+$ denotes the pseudoinverse, $\mathbf{I}$ is the identity matrix and $\mathbf{y}$ is a real-valued vector the same size as $\mathbf{x}$ that will be determined by an optimization procedure under the condition

$$\mathbf{y} = arg\ min \sum_i |\mathrm{d}_i| \tag{8}$$

Note that use of $\mathbf{y} = 0$ in Equation (7) leads to the usual pseudoinverse solution, which, as known, is the solution that minimizes the $L_2$-norm (thus obtaining a solution where displacements are minimal but affecting all points). Contrariwise, minimization of the $L_1$-norm entails the confinement of displacement values, although possibly large, within the least number of affected points.

In the case of the UPV calibration network, we have no strong reason to expect that displacements occur only in a little number of points. Quite the opposite, the hypothesis of small displacements affecting, if any, the majority of

**Table 10:** Coordinate displacements under the hypothesis of maximum number of stable points (mm).

| Coordinate | 12−13 | 13−14 | 14−15 | 12−14 | 13−15 | 12−15 |
|---|---|---|---|---|---|---|
| X1 | 0.00 | 0.00 | 0.00 | 0.00 | 0.00 | 0.00 |
| Y1 | 0.00 | 0.00 | 0.00 | 0.00 | −0.18 | −0.13 |
| X2 | 0.86 | 0.05 | 0.06 | 0.73 | 0.45 | 1.12 |
| Y2 | 0.00 | 0.00 | 0.00 | 0.00 | 0.00 | 0.00 |
| X3 | 0.00 | −0.39 | 0.00 | −0.24 | 0.00 | 0.00 |
| Y3 | 0.00 | 0.00 | 0.00 | 0.00 | 0.00 | 0.00 |
| X4 | 0.29 | 0.00 | −0.09 | 0.37 | 0.00 | 0.29 |
| Y4 | 0.00 | 0.00 | 0.00 | 0.00 | 0.00 | 0.00 |
| X5 | −0.01 | −0.89 | 0.00 | −0.96 | −0.76 | −0.88 |
| Y5 | 0.00 | 0.00 | 0.00 | 0.00 | 0.00 | 0.00 |
| X6 | 0.00 | 0.30 | 0.00 | 0.47 | 0.34 | 0.31 |
| Y6 | 0.00 | 0.00 | 0.00 | 0.00 | 0.00 | 0.00 |
| X7 | −0.86 | 0.00 | −0.28 | −0.60 | −0.02 | −0.98 |
| Y7 | 0.00 | 0.00 | 0.00 | 0.00 | 0.00 | 0.00 |

points may be the most plausible hypothesis for the UPV baseline. However, we want to analyse the deformation results under this new hypothesis since it will complement the conclusions obtained by the standard geodetic method and, in particular, will serve to reinforce the conclusions drawn about the most stable points to be used for GNSS absolute length research.

Table 10 shows the coordinate displacements obtained for the different campaign pairs under the maximum number of stable points hypothesis.

As it can be seen the method does not succeed in finding significant y-displacements for the given geometry whereas the largest x-displacements agree quite well, being usually larger, with those obtained by the traditional geodetic approach (Table 4).

# 7 Conclusions

First of all, both deformation monitoring methods show clearly that accurate determination of displacements in the y-coordinate, especially in pillars 2 and 7, is almost impossible due to the non-favourable geometry of the UPV network.

According to the traditional geodetic approach, a displacement over 1 mm in pillar No. 7 is detected. This displacement may be not very significant since lines 3–7, 6–7, and specifically 1–7 where only forward measurements can be done, are less accurate owing to limitations in

modelling refraction errors. Additionally, pillars No. 2 and No. 5 seems to have been displaced some 0.8 mm when they are compared with the first campaign in 2012, though no displacement can be detected between 2014 and 2015, where the same equipment was used.

Regarding the maximum number of stable points approach, the most significant displacements coincide with those deduced by the standard geodetic method: some 0.9 mm for the X2 between 2012 and 2013, some −0.9 mm for the X7 between 2012 and 2013 and some −0.9 mm for the X5 between 2013 and 2014. These are to be regarded as maximum displacements, i. e. they represent the order of maximum displacement for a few unstable points provided the majority of points remained stable. True figures have to be of the order or below these values, and the results obtained by the traditional geodetic approach also point to this conclusion.

In any case, both approaches come to the conclusion that pillars No. 1 and No. 3 are among the most stable in the baseline. Since the displacements obtained for them are minimal and little significant, they were selected for GNSS absolute length research.

Besides, it has to be acknowledged that most calibration baselines have been designed to comply with the ISO 17123(4) standard and are made up with aligned distances only. Their augmentation by means of external (not aligned) pillars is recommendable in order to improve the geometry for a better determination of possible pillar displacements, which, in turn, need to be determined along with uncertainties that have to be taken into account in the total uncertainty budget.

Finally, it has to be highlighted that the power of separability of the scale correction from individual pillar displacements increases with the baseline length. In the present case, where the baseline is relatively short, 330 m, uncertainties of few tenths of a mm in the distances can easily have an impact of 1 ppm in the scale correction.

# References

[1] Baselga, S., García-Asenjo, L. and Garrigues, P. (2013) Submillimetric GPS distance measurement over short baselines: case study in inner consistency *Meas. Sci. Technol.* 24 075001.

[2] Baselga, S., García-Asenjo, L. and Garrigues, P. (2015a) Deformation monitoring and the maximum number of stable points method. *Measurement*, 70: 27–35.

[3] Baselga, S., García-Asenjo, L. and Garrigues, P. (2015b) 'Submillimetric GNSS Distance Determination for Metrological Purposes'. *Proceedings of the 5th International Colloquium Scientific and Fundamental Aspects of the Galileo Programme* (downloadable at http://congrexprojects.com/2015-events/15a08/).

[4] Bell, B. (1992). Proc. Workshop on the Use and Calibration of the Kern ME5000 Mekometer. Stanford Linear Accelerator Center, Stanford University, USA, 18–19 June, pp. 1–80.

[5] Berné, J. L., Revhaug, I., Garrigues, P., García-Asenjo, L., Baselga, S. and Navarro, S. (2008) Calibration baseline at the Universidad Politcnica de Valencia: description and observation. Int. Congress on Geomatic and Surveying Engineeering (Valencia, Spain, 18–21 February 2008).

[6] Caspary, W. F. (1987) Concepts of Network and Deformation Analysis (School of Surveying, The University of New South Wales, Australia), Monograph 11.

[7] Denli, H. H. (2003) Global congruency test methods for GPS networks. *J. Surv. Eng.* 129(3), pp. 95–98.

[8] Grafarend, E. W., Sansò, F. (1985) Optimization and design of geodetic networks (Springer-Verlag).

[9] Heunecke, O. (2012) Auswertung des Ringversuchs auf der neuen Kalibrierbasis der UniBw Mnchen zur Bestimmung der Sollstrecken Allgemeine Vermessungs-Nachrichten (AVN). 119 (11–12), pp. 380–385.

[10] Heister, H., Heunecke, O., Liebl, W. and Neumann, I. (2011) Conception and realization of the new universal calibration baseline. *3rd Workshop on Absolute Long Distance Measurement in Air* (Prague, Czech Republic, 27 May 2011) (http://www.longdistanceproject.eu).

[11] ISO 17123-4 Field procedures for testing geodetic and surveying instruments – Part 4: Electrooptical distance meters (EDM) Optics and optical instruments.

[12] Jokela, J., Häkli, P., Ahola, J., Buga, A. and Putrimas, R. (2009) On traceability of long distances. *Proc. 19th IMEKO World Congress Fundamental and Applied Metrology*. (Lisbon, Portugal, 6–11 September) pp. 1882–7.

[13] Jokela, J. and Häkli, P. (2010). Interference Measurements of the Nummela Standard Baseline in 2005 and 2007. Publications of the Finnish Geodetic Institute. No. 144.

[14] Jokela, J., Häkli, P., Kugler, R., Skorpil, H., Matus, M. and Poutanen, M. (2010) Calibration of the BEV geodetic baseline. *FIG Congress 2010.* pp. 2873–87.

[15] Koivula, H., Häkli, P., Jokela, J., Buga, A. and Putrinas, R. (2013) GPS metrology:bringing traceable scale to local crustal deformation network *Geodesy for Planet Earth* (Int. Association of Geodesy Symp. 136) pp. 105–112.

[16] Lassila, A., Jokela, J., Poutanen, M. and Jie, X. (2003). Absolute calibration of quarz bars of Väisälä interferometer by white light gauge block interferometer. *17th IMEKO World Congress, Metrology in the 3rd Millenium* (Dubrovnik, Croatia, 22–27 June) pp. 1886–90.

[17] Neuner, H., Paffenholz, J. A. (2012) Bestimmung der Kalibrierbasis der UniBw Munchen mit dem Mekometer ME5000. Beitrag des Geodtischen Allgemeine Vermessungs-Nachrichten (AVN). 119 (10): pp. 344–346.

[18] Niemeier, W. (1981) Statistical tests for detecting movements in repeatedly measured geodetic networks. *Tectonophysics* 71: pp. 335–351.

[19] Pollinger, F., Meyer, T., Beyer, J., Doloca, N., Schellin, W., Niemeier, W., Jokela, J., Häkli, P., Abou-Zeid, A. and Meiners-Hagen, K. (2012) The upgraded PTB 600 m baseline: a high-accuracy reference for the calibration and the development of long distance measurement devices *Meas. Sci. Technol.* 23 094018.

[20] Rüeger, J. M. (1996) Electronic Distance Measurement (Springer).